Mapping Grip Force to Muscular Activity Towards Understanding Upper Limb Musculoskeletal Intent using a Novel Grip Strength Model

Yujun Lai, *Student Member, IEEE*, Elvera Abdel-Messih, Marc G. Carmichael, *Member, IEEE*, and Gavin Paul *Member, IEEE*

***Abstract*— This study aims to evaluate a grip strength model designed to elucidate the relationship between measured grip force and muscular activity and assess its impact on an upper limb musculoskeletal model. This work aims to develop the grip strength model by utilizing a piecewise linear function based on the Woods and Bigland-Ritchie EMG-force model, which derives its parameters from 10 adult participants performing isometric and dynamic gripping tasks. Experimental results demonstrate the model's efficacy in estimating surface electromyography (sEMG) readings from force measurements, with a mean root mean square error (RMSE) of 0.2035 and a standard deviation of 0.1207. Moreover, incorporating sEMG readings associated with grip force does not significantly affect the optimization of muscle activation in the upper arm, as evidenced by kinematic data analysis from dynamic tasks. This validation underscores the model's potential to enhance musculoskeletal model-based motion analysis pipelines without distorting results. Consequently, this research emphasizes the prospect of integrating external models into existing human motion analysis frameworks, presenting promising implications for physical Human-Robot Interactions (pHRI).**

***Index Terms*— Grip Strength Model, Human Motion Analysis, Musculoskeletal Model**

I. Introduction

The increasing ubiquity of robots in our everyday lives is a catalyst for the current shift in research towards Human-Robot Interaction (HRI), a field of research exploring the relationship between humans and robots in collaborative and cooperative scenarios [1]. The evolution of interactive systems that capitalize on human physiological signals for intent detection underscores their utility in HRI. Prior work [2] explored the inertia effects in Fitts' law tasks within interactive environments, highlighting the nuanced ways in which human intent can manifest through muscular activity. Similarly, gamification strategies have been employed to enhance user engagement and performance in these settings [3], which provided insights into human response in interactive systems. As newer robots enable humans to safely interact with the system in close proximity, there is a focal shift towards a better understanding of the human partner's intentions and reactions. The predominant approach to infer human intent is through the integration of human physiology in collaborative workspaces. Common methods include using physiological responses, such as bio-potentials, to deduce intent, provide feedback to the user, and hence maximize control during HRI. Commonly, this results in models that map electromyographic (EMG) [4] or electroencephalographic (EEG) [5] signals to user intention and performance.

Some frequency-domain and time-frequency-domain features have been reported to achieve good performance in detecting muscle co-contraction and predicting overall muscle strength. A part of the experimental methodology with sEMG is the variability introduced by both the users and the operators. Hudgins et al. [6] explored this effect of noise by using such frequency-domain and time-frequency-domain features to achieve a desired classification outcome for the specific actions based on EMG signals. In their study, only one pair of electrodes were used to record EMG signals, providing insufficient sEMG features and making it challenging to accurately pinpoint the most active muscle positions. Additionally, the electrodes were shifted in each experiment, creating variability. This underscores one current challenge: employing numerous sensors and electrodes may introduce inaccuracies over time. In addition, Bai et al. showed that rather than using high density sEMG data, it is possible to achieve the same accuracy with as little as 5 active signal channels [7]. Hence lies the challenge for building a model for detecting muscle activity using sEMG. Such a model should be capable of identifying upper arm intent, mitigating the need for additional sensors.

A holistic perspective towards human physiology-driven robotics can be achieved by utilizing neuro-musculoskeletal (NMS) models. NMS models, commonly referred to as musculoskeletal models (and referred hereon as such), have long been used to simulate anatomy and physiological responses. More recently, their potential to tackle human-centric robotics is realized with works leveraging the model's results for robotic assistance [8], [9].

With multiple confounding factors affecting human motor control [10], learning [11], and planning [12], musculoskeletal

Manuscript submitted: xx/04/2024. All authors are with the UTS Robotics Institute (UTS:RI), University of Technology Sydney (UTS), Sydney, Australia. (*Corresponding author: Elvera Abdel-Messih*)

models have been invaluable for researchers to isolate and investigate their influence on human response. The fidelity of musculoskeletal models in representing human muscular activity is pivotal for their application in predictive models of human behavior. Recent work by Sutjipto et al. [13] introduces a novel representation of strength profiles, offering a more granular understanding of the relationship between grip strength and muscle activation. This advancement is crucial for refining musculoskeletal models to better predict human physiological responses in dynamic tasks.

Despite being a tertiary source of information, grip strength has the advantage of overcoming biases associated with surface EMG (sEMG) readings, especially with dynamic movements, which are particularly challenging for sEMG-based models. Additionally, they can be computationally accounted for as defined by the musculoskeletal models.

This work aims to build a grip strength model based on the Woods and Bigland-Ritchie model to correlate the relationship between grip strength and muscular activity. Such a model may alleviate the need for extraneous sensors to be attached to the human user, allowing for seamless integration of extrinsic information channels into the human motion analysis pipeline. Experimental data will validate the grip strength model, using measured grip force and sEMG signals as analogs of grip strength and muscular activity. The influence of the grip strength model on a typical human motion analysis is investigated through a commonly used musculoskeletal model [14], [15].

The rest of the article is as follows: Section II introduces and explores musculoskeletal models and their relationship with grip strength models, then Section III outlines the experiment methodology to create and validate the grip strength model, with results presented in Section IV. A discussion on the implications of the results follows in Section V, followed by the conclusion in Section VI.

II. Background

Musculoskeletal models are created to act as analogs for biological systems and use physics-based simulations to investigate anatomical and muscular responses to input stimuli. With a variety of software available for simulations [16], [17], there is a significant body of work focusing on feature comparison [18]–[21] and real-world phenomenon validation [22]. However, there are many roadblocks in adopting musculoskeletal models in certain applications.

While simplified models can contribute towards a deeper understanding of the human central nervous system and physiological interactions, realistic analogs are hampered by the complexity of the human body. Intricate body systems, such as the upper limb complex, translate to complicated models that are challenging to validate [23]. Realistic models also pose a conundrum for researchers due to the kinematic redundancy between the number of muscles and the unconstrained Degrees of Freedom (DoF), an advantageous feature for human dexterity and adaptation [24]. With no closed-form solutions available to obtain muscular activity for a particular state, optimization-based solutions are currently the favored approach to resolving this redundancy. However, there is an ongoing debate on the appropriate cost function to be used during this optimization, with arguments for [25] and against [26] using principles of optimal control.

The most widely accepted cost function to determine muscle activation relies on the principle of minimum energy expenditure [27], deriving the minimization of the sum squared muscle activation. However, evidence suggests that this is not as relevant even for elite athletes whose successes rely on optimizing their actions [28]. Additionally, an energy expenditure-centric approach fails to consider compensatory energy usage in populations such as the elderly [29] and those with a lack of proprioceptive input such as deafferented individuals [30]. Furthermore, muscular co-contraction, a critical characteristic for human motor learning [31], is not considered when using minimum energy expenditure principles. The effect of muscular co-contractions can be seen in the regulation of body segment impedance [32], accuracy [33], and task variability [34], which highlights current limitations.

A possible solution to tackle current limitations is integrating novel information available through emergent technologies. These aim to supplement or supplant parameters and functionalities of musculoskeletal models using extrinsic channels of information, such as camera-based 2D & 3D human pose estimation [35], marker-less motion capture systems [36], and IMU-based motion analysis [37].

Following the same line of thought, models that bridge the gap between task-centric measures and physiological states can complement musculoskeletal models. Such models incorporate some form of physical contact between the human and the robot, especially for physical HRI (pHRI) applications. A handle is commonly used to facilitate end-effector-based interactions [38]. Besides the interaction forces at the end-effector, the grip strength on the handle can be used as a channel of information, similar to kinematic velocities during unconstrained voluntary point-to-point movements [39].

Human grip strength has been well studied with excellent inter-rater and test-retest reliability [40]. Early studies have shown its links to the somatosensory system [30], with pressure distribution dynamics investigated by Gurram et al. [41].

The use of grip strength provides the opportunity for a model that maps the relationship between grip strength and muscle activation for the relevant muscle groups. Finger flexion and extension are attributed to the *flexor digitorum profundis* (FDP) and *extensor digitorum communis* (EDC) muscle groups [42], with the FDP muscle group being the primary contributor to human grip force.

In pHRI applications, grip strength has been used to indicate human physiological response to perturbations [44]. Still, the inherent variability among human demographics creates a challenge for intent detection and human-robot role arbitration [45]. Human performance can vary based on psychological and physiological characteristics, and thus, alternative perspectives on inferring intent are necessary to provide robust solutions.

One popular model hypothesized for the relationship between muscular activity (% normalized EMG) and force generation (% MVC) is the two-element model by Woods and

Bigland-Ritchie [43], which suggests that there are intrinsically two types of muscle fibers during muscle activation (see Fig. 1). This model is supported empirically [46] while De Luca et al. identified that the curve parameters are unique to each muscle group [47]. Assuming that the slow Type 1 fibers generate force asymptotically at 30% of MVC, the Woods and Bigland-Ritchie model can be parameterized using piecewise equations to isolate the two fiber types.

III. Experiment Methods

The experimental method was composed of three types of trials: a reference trial, isometric trials and excerise trials. The reference trial was used for MVC, the isometric trials were used to construct the grip strength model, and the excersise trials were used to validate the model. The isometric trials were randomised between 33%, 66% and 100% to and the original aim was to affirm MVC - but this was not possible when the data was sorted.

A series of double-blind, randomized trials were conducted to obtain each participant's isometric and dynamic grip force across three voluntary contraction levels: 33%, 66%, and 100%. A set of standardized verbal instructions was provided to participants, with participants instructed to maintain 90° elbow flexion, no radial/ulnar deviation of the wrist, and a natural grasp on the handheld dynamometer. Across all participants, the estimated wrist extension was within $\pm 15°$ with no significant changes throughout the experiment.

The experiment consisted of one reference trial, 12 isometric trials, and 6 exercise trials. In each trial, the grip force exerted by the participant was measured by a digital dynamometer ($\pm 0.1kg$). The measurements from the digital dynamometer were captured using video footage and extracted manually post-hoc. Administrators advised participants against reading their grip force results after each trial, although no physical restrictions were employed to enforce this. For all trials, the maximum grip force measurement was collected. This aligns with the sEMG data processing pipeline (Section III-E) to extract the maximum Root Mean Square (RMS) values.

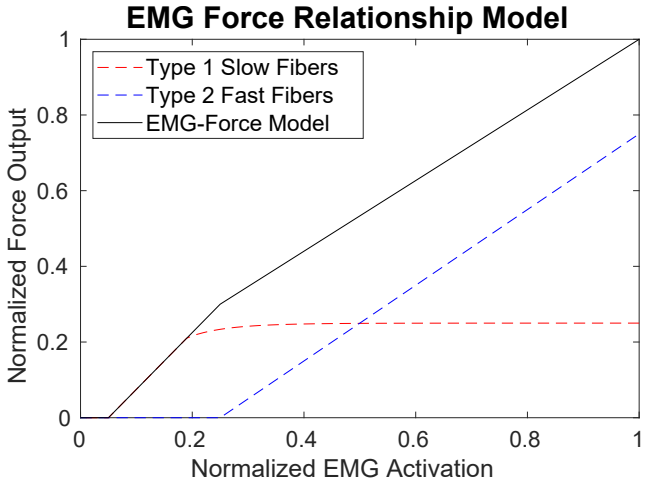

Fig. 1: The two-element EMG-Force model proposed by Woods and Bigland-Ritchie used for the grip strength model (reproduced from [43]).

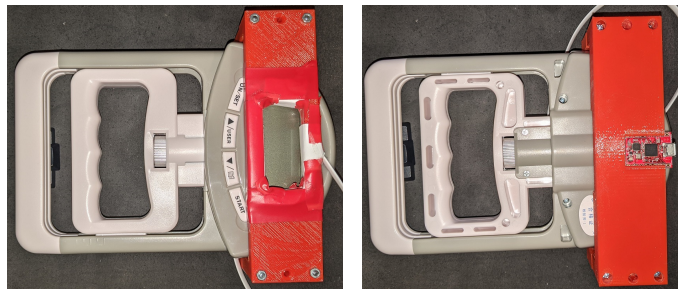

(a) (b)

Fig. 2: The front and back views of the digital dynamometer fitted with a 3D printed part to house (a) the diffused LED light strip, and (b) the attitude and heading reference system (myAHRS+).

TABLE I: The targeted muscle groups for the placement of the sEMG electrodes.

Electrode Number	Muscle Group	Muscle Acronym
1	Extensor Digitorum Communis	EDC
2	Flexor Digitorum Profundus	FDP
3	Biceps Brachii	BIC
4	Triceps Brachii	TRI
5	Deltoideus Posterior	DELT1
6	Deltoideus Medius	DELT2
7	Deltoideus Anterior	DELT3

In the reference trial, participants were instructed to "squeeze as hard as possible for 5 seconds while maintaining your trunk and arm posture". They were further instructed to "use this [*reference trial*] to relate to the 33% and 66% grip strength level for the rest of the experiment". The participants approximated the 33% and 66% grip strength levels to the best of their ability. No further feedback was provided to the participants for the rest of the experiment.

A. Participant Measurements and Sensor Placement

Prior to the recorded trials, the length of each participant's ulna and humerus were measured using identical protocols as those from the CDC (US) [48] and the NHS (UK) [49].

Muscular bio-potentials are collected through silver-silver electrodes using the Delsys Bagnoli 8-Channel system (Delsys, Natick, MA). Electrodes are positioned based on SENIAM guidelines[1], targeting muscle groups listed in Table I.

Motion capture software was utilized to track the kinematics of each participant's upper limb. A total of 12 Optitrack Prime cameras, in conjunction with the Motive software (NaturalPoint, Corvallis, USA), tracked four user-defined rigid body assets (Fig. 4). Each rigid body asset consists of 3 passive reflective markers with known locations to provide unique poses. The rigid body assets are placed to coincide with the 4 major body segments of the model: chest (thorax), upper arm (humerus), forearm (ulna), and hand (lunate).

[1] http://www.seniam.org/

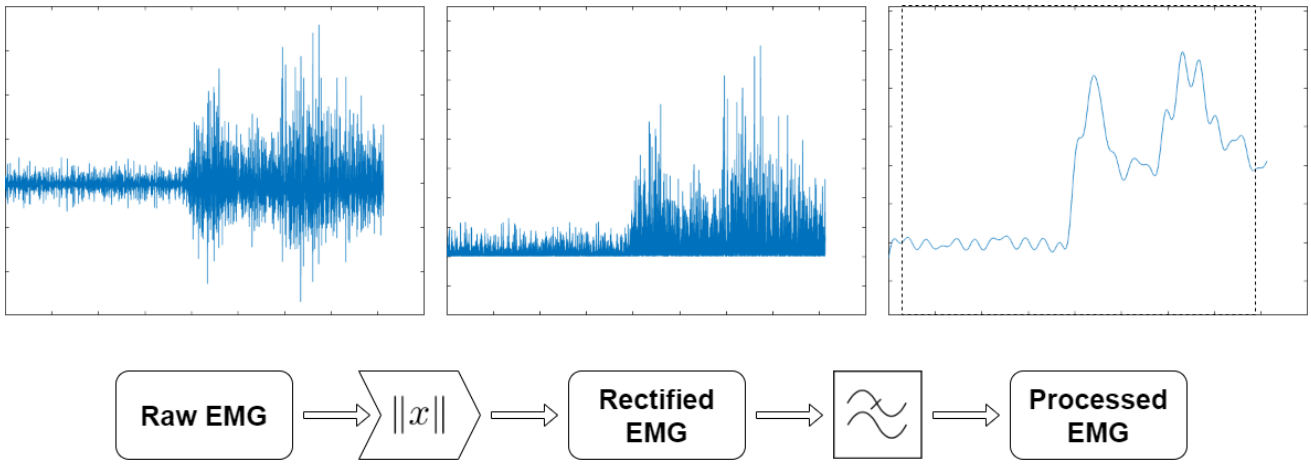

Fig. 3: An illustration of the sEMG processing pipeline.

B. Isometric Trials

Participants were requested to maintain the arm and trunk posture for isometric trials as shown in Fig. 4. In each trial, participants were given a 5-second visual countdown, after which participants were instructed via visual instructions to squeeze the dynamometer for 5 seconds at 3 distinct strength levels: 33%, 66%, and 100%. Between each trial, participants were given a one-minute break to mitigate muscular fatigue arising from the experiment.

Each participant performed 4 trials per grip strength level, with the order of the 12 trials randomized using Latin squares. The grip strength level for each trial was occluded from the administrator using a screen not visible to the administrator. For each isometric trial, sEMG data collection commenced 2 seconds into the countdown, resulting in 8 seconds of data for each trial.

C. Exercise Trials

At the start of the exercise trials, participants were instructed to watch a video that shows a reaching exercise[2]. The exercise trials were performed in a darkened room to reduce reflections from the passive reflective markers. Thus, LED light strips were diffused and attached around the LCD display of the digital dynamometer to facilitate the reading of the grip force measurements on the video footage (see Fig. 2(a)).

Similar to isometric trials, visual instructions for the grip strength levels were given to participants. They were verbally instructed to "squeeze at the indicated grip strength level and start your [*sic*] movements while maintaining your [*sic*] trunk posture". No further requirements, such as task completion speed or accuracy, were imposed on participants.

Kinematic data for participants are collected from the exercise trials using the rigid body assets, starting when the countdown commences. Since there were no task completion speed requirements imposed, participants were instructed to indicate to the administrator verbally when they "feel like you [*sic*] have completed the exercise from the video". Similar to the isometric trials, sEMG data collection commences 2 seconds into the countdown. Both sEMG and kinematic data collection are stopped manually by the administrator when they receive participants' verbal indication.

Both kinematic and sEMG data from the exercise trials are used for post-hoc analysis with the musculoskeletal model. External forces exerted on the participant's hand are calculated from linear acceleration readings from an attitude and heading reference system (WITHROBOT, Seoul, Korea), along with the mass of the sensor-equipped dynamometer ($m = 0.516kg$). Forces induced by gravity are also included in the dynamic analysis of the musculoskeletal model (Section III-G).

[2]The exercise video shown to participants is available here

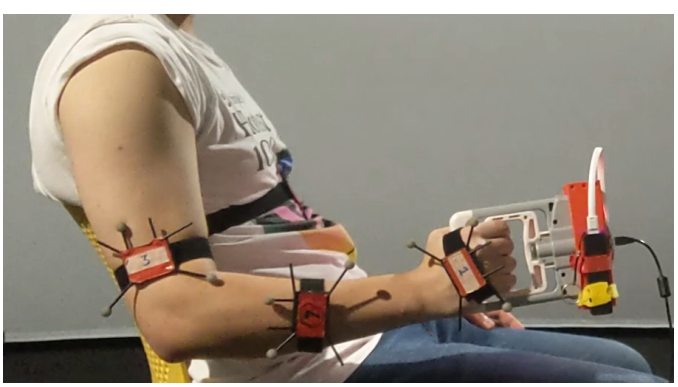

Fig. 4: The posture participants were requested to maintain during isometric trials. Four rigid body assets were attached to the arm (3) and torso (1) as a reference for the musculoskeletal model.

D. Incorporation of Muscle Fatigue Effects

Participants were provided with a minute break between each trial. However, the time provided to participants in prior works has varied from 90 seconds [50] up to 180 seconds [43]. Thus an investigation into the possible effects of muscle fatigue in the results was conducted.

The most common method is using Power Spectral Density (PSD) plots and investigating whether there has been a shift in the peak power frequency. The raw EMG signals from the experiment were analyzed using both Fast Fourier Transforms

and Welch Power Spectral Density estimate, functionalities performed using MATLAB's implementation (*fft* and *pwelch* functions, respectively). Gaussian smoothing with a window size of 40 was performed on the Welch PSD to obtain clear peaks of the PSD curve. For each trial, the EMG signals were segmented into three temporal sections, with the first section starting 0.5s after the visual instruction was provided to the participants.

E. sEMG and Kinematic Data Processing

The collected sEMG signals are rectified before applying a 4th-order Butterworth lowpass filter with a cutoff frequency of 4Hz. The first and last 0.5 seconds of the processed sEMG signals are ignored to remove artifacts arising from observations of partial phases. An overview of the sEMG processing pipeline can be seen in Fig. 3.

The grip strength model aims to build a mapping between muscular activity and the grip force exerted by each participant. The sEMG signals are normalized to allow for quantitative analysis between participants. A common method to normalize sEMG signals is to conduct Maximum Voluntary Contraction (MVC) trials, which aim to maximize the muscle activation of specific muscle groups. Despite ongoing work to determine the optimal set of exercises for inter-rater reliability and MVC values [50], different exercises are prescribed for different muscle groups.

F. Grip Strength Model

To construct the grip strength model mapping the relationship between grip strength output and muscular activity, isometric trial data from ll participants are used to generate and validate the model through exercise trials. To ensure the model's validity across all participants, both sEMG intensity and grip force are range-normalized.

While muscle force generation is constrained by their force-length-velocity (FLV) curves [51], which affect muscle moment arms, participants were instructed to maintain a static posture during the isometric trials (Section III-B), making the relative effect of the FLV curves negligible.

For the exercise trials, the grip strength model does not consider FLV curves, which may skew the results. An exploration of the effects from the FLV curves is conducted to ascertain the scale of this effect across different poses and velocities as extracted from participant kinematic data. Thus, to validate the model, the generated moment arms were compared in three phases of a reaching movement: a starting pose, an end pose, and an in-transit pose. The mean absolute difference of moment arms (41 muscles on 94 musculoskeletal model coordinates including the FDP and EDC muscle groups) between the starting pose and the other two was determined. These coordinates are local frames of references for the insertion points and bones. Joints provide the DoF and are separate entities to coordinates in opensim models.

In essence, the isometric trials were used to build the model, and the exercise trials were used to validate the model.

G. Musculoskeletal Model

The upper limb musculoskeletal model used for the experiments is derived from the Stanford VA Upper Limb model [14] with updated model parameters from live human data [15]. The model consists of 15 degrees of freedom and 50 Hill-type muscle-tendon units (MTUs) [52]. Modifications were made to the model to simplify the model while maintaining bodies, coordinates, and actuators relevant to the experiment. Updates to the model include[3]:

- Inertial properties of the humerus, radius, and capitate were set using anthropomorphic estimation for the average male height and weight [53]. Principal moments of inertia for the body segments are taken from [54].
- The MTU model of the original model [55], is replaced by the more recent [56] MTU model. Available MTU parameters are transcribed to the new MTU model (maximum isometric force, optimal muscle-tendon length, pennation angle at optimal length, tendon slack length). Other MTU parameters (Force-Length-Velocity curves) are set to the default values in OpenSim.
- The model complexity is reduced by restricting motion to 5 DoFs, comprising of: shoulder flexion/extension, abduction/adduction, internal/external rotation (3 DoF), elbow flexion/extension (1 DoF), and wrist flexion/extension (1 DoF). The remaining joints are locked to match the experiment posture (e.g., closed digits, neutral pronation/supination, and 0° wrist abduction/adduction). MTUs that do not contribute to the 5 DoFs are disabled by ignoring them during calculations. MTUs contributing to grip strength are not changed and matches those from the original model (EDC and FDP muscle groups).

For each participant, the measurements of their humerus and ulna are used to scale the geometry of the model manually. The length of the humerus and ulna matches their respective measurements, while the length of the radius is proportionally scaled based on the ulna measurement.

For each exercise trial, upper limb motion analysis is conducted by performing inverse kinematics, inverse dynamics, and kinematic analyses. All three operations utilize the functionalities in OpenSim.

The generalized forces obtained from inverse dynamics are used for static optimization in MATLAB (using the *fmincon* function) to obtain an estimate of the muscular activity, $\tilde{A}$, during the exercise trials. A minimum sum of squared activation cost function is used:

$$\min \sum_{i=1}^{M} a_i^2, \tag{1}$$

$$s.t. \qquad M(q)\tilde{A} = F, \tag{2}$$

where $M(q)$ is the moment arm matrix, which depends on the current joint state, F is the net generalized forces on the model joints, and $\tilde{A} = [a_1, a_2, \cdots, a_m]^T$ is the activation level $(0 \rightarrow 1)$ for the m MTUs in the model.

For the purpose of demonstrating the feasibility of integrating extrinsic information channels with musculoskeletal

[3]Updated model: https://github.com/y-lai/modifiedUpperLimbModel.

TABLE II: The replacement of the MTU activation in the musculoskeletal model with the model estimate.

Muscle Group	Model MTUs
EDC	EDCI, EDCL, EDCR, EDCM
FDP	FDPI, FDPL, FDPR, FDPM

models, the muscle activations for FDP and EDC are assumed to be identical (assuming isometric co-contraction). The muscular activity estimate is obtained using the normalized EMG readings of the FDP muscle group. Both values replace multiple MTUs in the musculoskeletal model as shown in Table II. The generalized forces caused by the EDC and FDP activation are considered when optimizing the remaining MTUs in the model.

IV. Results

Ten male adults presenting no neuromuscular disorders participated in the experiment. The experiment protocols were explained to the participants before obtaining their informed consent. This research has been carried out according to the ethical guidelines of the Human Research Ethics Committee at the University of Technology Sydney (UTS HREC approval no.: ETH18-3029).

From an initial analysis of the reference trials, the common method to normalize the sEMG readings was not followed as 6 out of the 10 participants demonstrated supramaximal sEMG readings during the isometric and exercise trials for electrodes 1 & 2. This is likely due to the lack of feedback provided to participants throughout the experiment.

Thus, a different normalization method is used based on the sEMG intensity range. Since participants were instructed to hold onto the handheld dynamometer (0.516kg) in a relaxed manner, the sEMG intensity for muscle activity during this time is assumed to be the minimum value.

The sEMG intensity is obtained by partitioning the signal into rolling windows which are 0.25s long (0.05s apart), and calculating the RMS for each window. Since the experiment includes an exercise suitable for MVC (e.g., 100% grip strength), each participant's normalization range is formed by the minimum RMS value between 0.5-3.0s and the maximum RMS value across all trials.

The sEMG signals from electrode numbers 3–7 were not processed since they are used for qualitative analysis with the static optimization results.

A. Contribution of Muscle Groups

The generation of human grip strength is attributed to the muscle groups that control finger flexion and extension: FDP and EDC. To ascertain the influence of each muscle group on a user-generated grip force, a series of one-way ANOVA was conducted between each muscle group and their relationship to the measured grip force.

Only the subset of isometric trials where participants were instructed to exert at 100% grip strength was used in this particular analysis, with the muscular activity posited to be a better representation of grip strength. Isometric trials for 33% and 66% grip strength are assumed to incur influence on muscular activity as participants try to control and maintain the instructed grip strength level. This can be seen in Fig. 5, where there is a larger spread of muscular activation despite a smaller grip force spread.

The normalized EMG activation of FDP and EDC are statistically the same ($F(1, 54) = 1.0570, p = 0.3085$), with no significant difference during 100% isometric trials. This is reinforced by the Pearson and Spearman's Rank Order correlation score, which shows a relatively equal correlation between each muscle group and the measured grip force as outlined in Table III.

Given the comparable correlation between measured grip force and the FDP and EDC muscle groups, the decision was made to adopt a single-variable model. The preference for utilizing the FDP muscle group is attributed to its broader sEMG signal range during contractions, facilitated by range normalization of the signals. Using a higher range mitigates the effects of signal noise, alleviates the chances of supramaximal and negative EMG activation, and accommodates a diverse participant pool with varying muscular strengths.

TABLE III: Correlation scores between EDC, FDP, and grip force. Pearson's correlation scores are in the top right triangle, while the lower left triangle shows Spearman's Rank Order correlation score.

		EDC Muscle	FDP Muscle	Grip Force
		Pearson's ρ		
EDC Muscle	Spearman's ρ		0.5961	0.7280
FDP Muscle		0.5644		0.7675
Grip Force		0.7203	0.6776	

B. Grip Strength Model Validation

The sEMG readings for two participants were observed to have no visible artifacts from muscle activity present across all trials and were unused in further analyses. The lack of visible artifacts derives from a flat-line response from the sEMG readings. This indicates an erroneous application of the electrodes during the setup process.

Further visual inspection of the data from isometric trials (Fig. 6) highlighted outliers. An initial analysis was conducted to determine the impact of the outlier.

Visual observation of grip force vs. FDP activation in Fig. 6 indicates that two additional participants' data are outliers. The RMS error between the isometric trial data and model was calculated by building a step-wise linear regression model (*stepwiselm* function in MATLAB) from the remaining data. The error was more than 3 times the standard deviation of the mean RMSE. Building the grip strength model with the remaining participants resulted in a mean RMSE $\mu = 0.1512$ with a standard deviation of $\sigma = 0.1207$.

The grip strength model was validated using the results from the exercise trials (Fig. 7), showing a mean RMSE of $\mu = 0.2035$ with a standard deviation $\sigma = 0.1207$. While evidence

suggests a power curve would fit a similar relationship [41], this was not investigated in this work. A comparison between the instructed grip strength level and the measured grip force suggests a similar relationship as shown in Fig. 8. However, multiple confounding factors can be attributed to the observed trend in Fig. 8, but this is outside the scope of this work.

For the three poses evaluated, the mean absolute differences in moment arms between the starting pose, and the ending and in-transit poses are $\mu_{end} = 1.6913$ (3.76% of the total) and $\mu_{transit} = 1.2963$ (2.82% of the total), respectively. This showed that particpants' moment arm differences is negligible.

C. Impact of sEMG Data Inclusion on Muscle Activity Estimates in Grip Strength Modeling

A series of optimizations using MATLAB's *fmincon* function were conducted to investigate the influence of the grip strength model's estimates on resultant muscle activity. The cost function for the optimization follows the default used in OpenSim, the minimum sum squared value of the muscle activation. Due to the use of minimization during the optimization process, the resultant muscle activity is generally underestimated when compared to empirical data. The discrepancies seen in Fig. 9 for the FDP and EDC muscle groups can be attributed to the range normalization process for the sEMG readings and implicit errors in the process of data collection. Moreover, simplified external load estimates from the dynamometer may not fully account for participant compensatory behaviors.

Figure 9 provides a visual contrast between scenarios with sEMG data inclusion and those without, particularly noticeable in muscle groups such as FDP and EDC. This distinction underscores the significant role that sEMG data plays in refining the accuracy of muscle activity predictions. Notably, the variations in muscle activity over time, as illustrated, offer a nuanced understanding of the dynamic interplay between different muscle groups during grip strength exertions.

The inclusion of sEMG data significantly enhances the model's sensitivity to muscle activation patterns, particularly within the FDP and EDC muscle groups, as evident in the pronounced activity profiles displayed in the figure. This enhancement demonstrates the value of sEMG data in capturing the complex dynamics of muscle activity during grip tasks, despite the challenges of range normalization and potential measurement errors. The observed discrepancies between em-

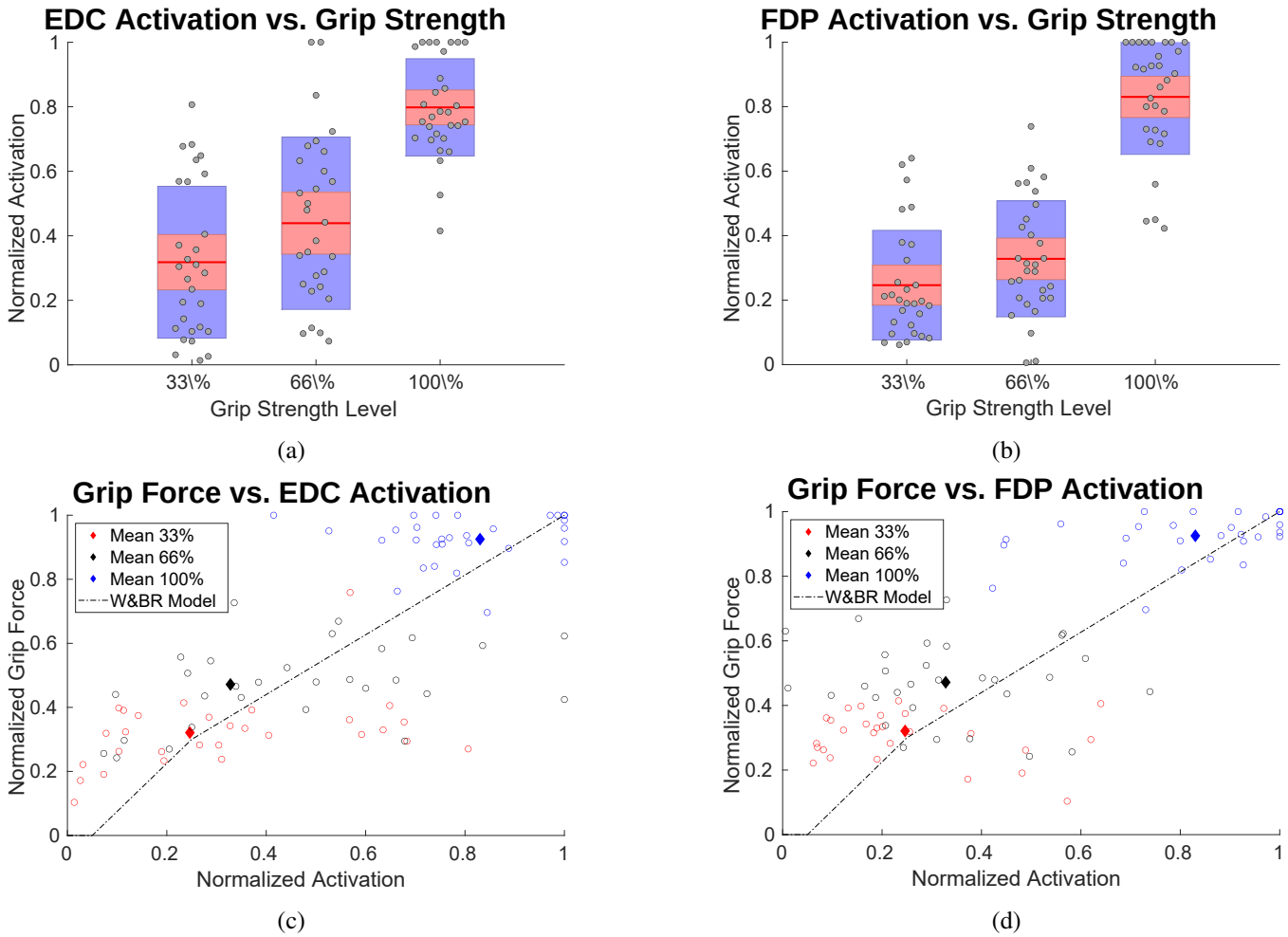

Fig. 5: The relationship between the grip force measurements and muscle activation for all participants in the experiment. The Woods and Bigland-Ritchie muscle EMG-force model is given as a reference.

pirical data and model estimates highlight the important role of accurate sEMG integration in improving muscle activity modeling.

D. Assessment of Muscle Fatigue Effects

The PSD plots across the three temporal sections for all participants indicated that acute effects of muscle fatigue are present within each trial (Fig. 10). This phenomenon is expected as participants are instructed to exert grip force for at least 5 seconds in each trial. Thus, to assess the longer-term effects of muscle fatigue, only the first temporal section of each trial was used for analysis.

For each participant, the first and last two 100% strength level trials (across both isometric and exercise trials) were used to perform a one-way ANOVA analysis. For both FFT-derived and Welch PSD estimates, there was no significant shift in the peak frequency (FFT: $F(1,38) = 0.9943, p = 0.3250$, Welch: $F(1,38) < 0.001, p = 0.9823$), indicating that the effects of muscle fatigue are negligible in the experiment.

V. Discussion

From the experiment's sample size, the generated grip strength model has proven to be a feasible adjunct for estimating EMG activation based on measured grip force. Despite utilizing data from only 10 participants, the correlation between each muscle group and the measured grip force aligns with the Woods and Bigland-Ritchie model, as illustrated in Fig. 5. The current understanding of FLV constraint effects on MTUs is well-documented [51] and the effects can be treated as negligible. Empirical visual observations further corroborate that the Woods and Bigland-Ritchie model can effectively link EMG activation with grip force.

Visual inspection of isometric trial data (Fig. 6) revealed outliers, suggesting potential experiment setup deficiencies. An initial analysis focused on the impact of these outliers, indicating an enhancement in model quality upon excluding certain data points. However, this study encountered a limitation due to data loss during retrieval. For some trials, the video footage of the experiment was underexposed, leading to an inability to read the measured grip force ($\sim 14\%$) from the video footage. Despite this, the analysis of the remaining dataset revealed a positive correlation between grip strength levels and normalized grip force. These findings affirm the model's validity, extending the Woods and Bigland-Ritchie model to represent sEMG activation to muscle fiber force output. The model can be extended to infer human intent, limiting the use of additional sensors—marking a novel contribution to the field.

Visual observations of Fig. 7 and Fig. 8 reinforce the relationship between the instructed or expected grip strength and the actual grip force measured during the exercise trials. Additionally, Fig. 7 suggests that the data from participants' exercise trials would fit the model. The collected data does not cover normalized forces < 0.3, so there is not enough

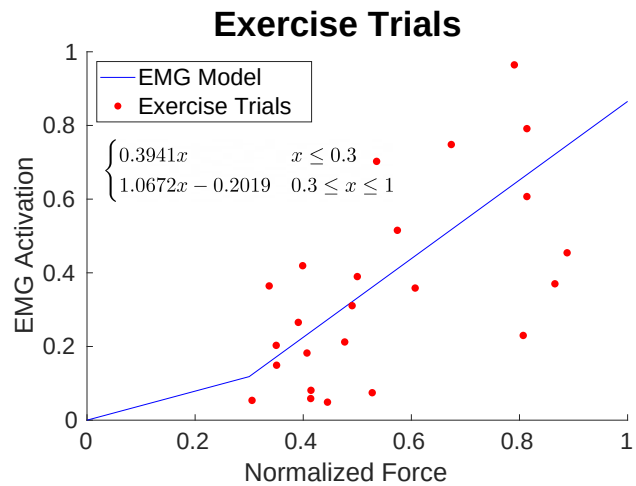

Fig. 7: Sample data from valid exercise trials and the parameterized grip strength model used for validation.

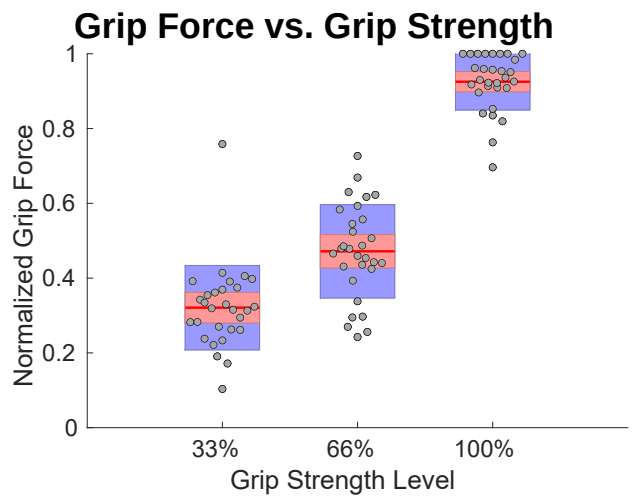

Fig. 8: A modified box plot of the instructed grip strength level and the measured grip force for all participants. The red line indicates the mean, the standard deviation is shaded in pink, and the 95% confidence interval is shaded in blue.

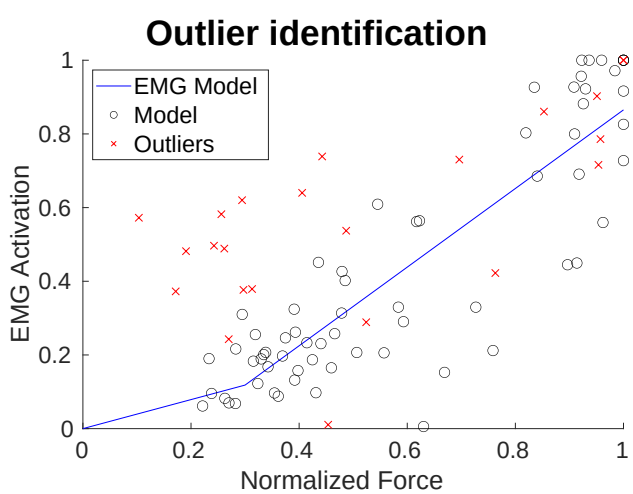

Fig. 6: A scatter plot of the sample points used for building the model and the outliers identified visually.

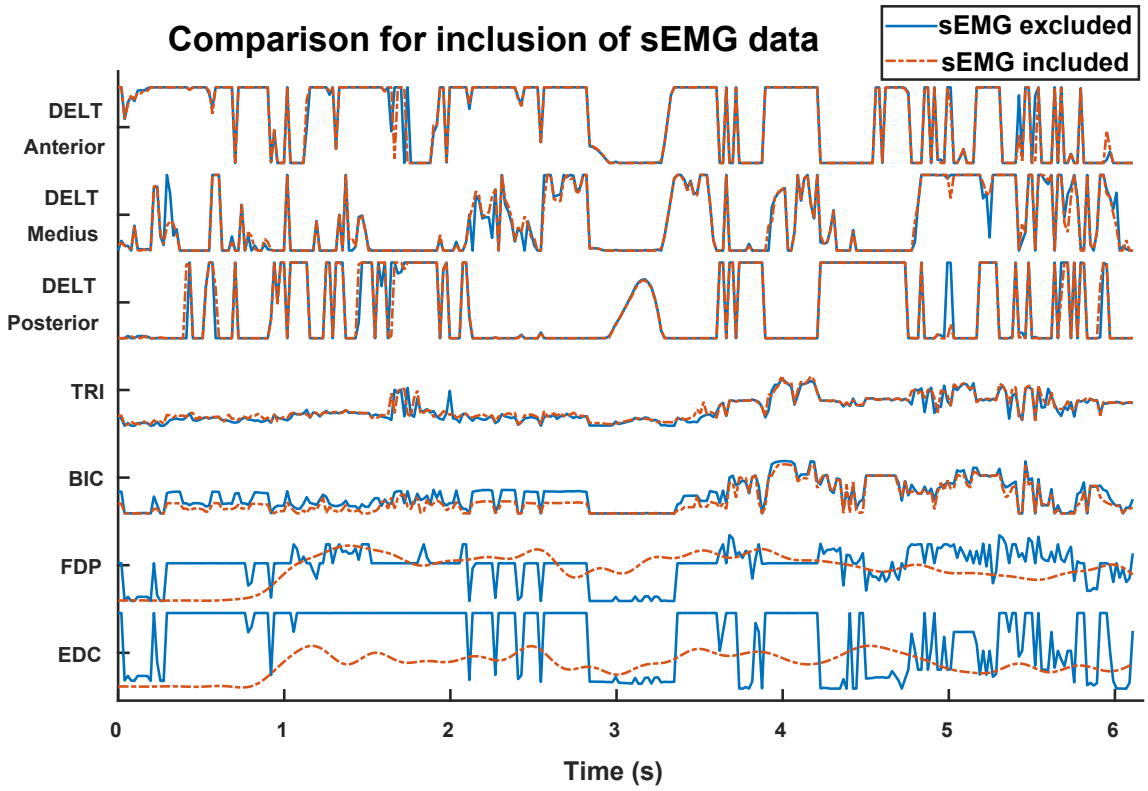

Fig. 9: A comparison of the effect of the grip strength model estimate on the EMG activation of the biceps, triceps, and deltoideus muscle groups.

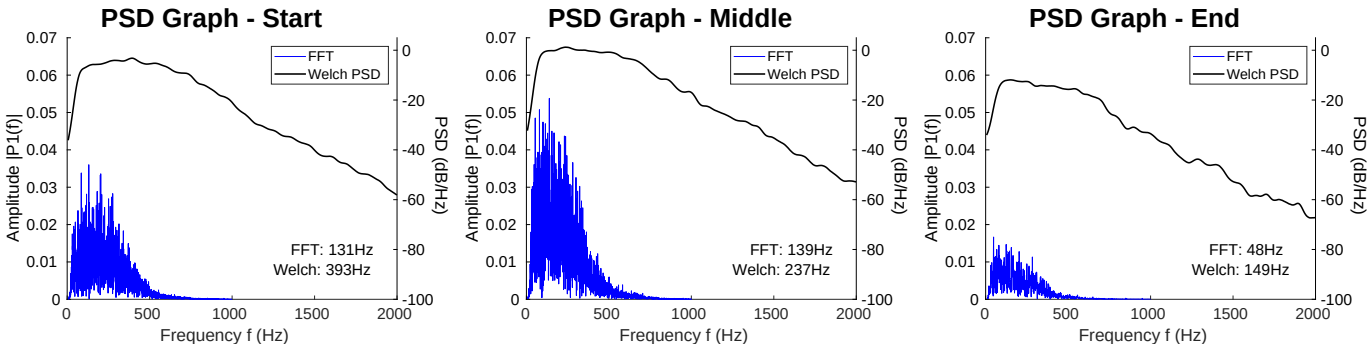

(a) (b) (c)

Fig. 10: The Power Spectral Density plots across (a) the first third, (b) the second third, and (c) the final third of a trial. These plots are representative of the PSD across most of the isometric and exercise trials.

data to firmly support the conclusion. However, the consistent and predictable pattern in the participants' responses validates the model to be used as an alternative to, or in conjunction with other models or in the future.

Although a set of electrodes and sEMG sensors were initially employed, the model's results indicate alternative sensors to sEMG systems can be utilised which are more practicable in pHRI applications. This highlights the model's capability to supplant traditional sensor-based measurements. This advancement simplifies experimental setups and opens new research methodologies where reliance on EMG or sEMG sensors can be reduced or eliminated. Further, this enhances efficiency and broadens the scope for future muscle activity measurement and modeling explorations.

The result in Fig. 9 indicated that including the grip strength model has not affected the functionality of the motion analysis pipeline for a musculoskeletal model for the muscles in the proximal sections of the upper limb. This supports the concept of employing a suite of discrete models that provide extrinsic channels of information to supplement musculoskeletal models during motion analysis. A notable phenomenon is that muscle activation from FDP and EDC may alleviate the activation necessary from biceps brachii to enable the recorded motion. This reinforces the previous observation of bias that may be introduced into musculoskeletal models by supplementary information sources and needs to be explored in future works

considering the applications of this model.

Considering the insights from the experimental results, where discrepancies in muscle activity estimation were observed due to the dynamometer's limitations and other factors, a potential improvement could be introduced. Implementing a lightweight force transducer in place of the dynamometer could mitigate the identified effect, enhancing the accuracy of the grip strength model's estimates and reducing the observed discrepancies in muscle activity. This adjustment suggests a pathway to refining the experimental setup for more precise and reliable outcomes.

The grip strength model aims to contribute to the current trend in generating supplementary information channels that complement musculoskeletal models. This will encourage their adoption in emerging fields such as rehabilitation [10], assessment [57], and pHRI [35]. While the grip strength model provides additional information sources when inferring human intent, such as in pHRI, it may introduce bias in the muscular activity analysis. Realistic musculoskeletal models are particularly sensitive to this possibility as the upper limb complex has complicated muscle-tendon paths.

Building on the foundation laid by this study, future endeavors could focus on refining and personalizing the grip strength model to cater more effectively to individual physiological variations. The prospect of tailoring the model using advanced computational techniques, such as machine learning algorithms or Bayesian statistics, presents an exciting frontier. This personalized approach would enhance the model's accuracy and applicability in diverse scenarios and open new pathways for integrating real-time physiological responses into comprehensive human motion analysis frameworks. Such advancements could improve the precision of assessments in rehabilitation and physical human-robot interactions, ensuring that the grip strength model evolves into an even more potent tool for predicting and understanding muscle activity.

VI. Conclusion

This work has successfully developed and validated a grip strength model that maps the intricate relationship between measured grip force and muscular activity. Through testing with 10 participants across a range of isometric and dynamic gripping tasks, the presented model has demonstrated accuracy in estimating sEMG readings from grip force measurements, with a mean RMSE of 0.2035 and a standard deviation of 0.1207. The findings validate the model's effectiveness in integrating with upper limb musculoskeletal analyses, confirming that the inclusion of sEMG data does not compromise the optimization of muscle activation or the overall outcomes of motion analysis. This achievement underscores the model's robustness and potential to augment musculoskeletal modeling by minimising sensory equipment.

Moreover, the application of the presented grip strength model in practical scenarios highlights its value in enhancing the precision of muscle activity estimations, particularly in the domain of pHRI. The model's capacity to infer upper muscle intent based on grip force alone, aligning with established EMG-force models, represents a significant stride toward more intuitive and accessible musculoskeletal analyses. Through examination and interpretation of experimental data, the assessment of muscle activity patterns, this work confirms the model's reliability and strategic relevance in the broader context of human motion studies. This approach paves the way for more sophisticated analyses that can contribute meaningfully to advancements in rehabilitation, assessment, and pHRI, affirming the grip strength model as a critical tool in the intersection of biomechanics and interactive technologies.

References

[1] D. P. Losey, C. G. McDonald, E. Battaglia, and M. K. O'Malley, "A review of intent detection, arbitration, and communication aspects of shared control for physical human–robot interaction," *Applied Mechanics Reviews*, vol. 70, no. 1, 2018.

[2] S. Sutjipto, Y. Lai, M. G. Carmichael, and G. Paul, "Fitts' law in the presence of interface inertia," in *2020 42nd Annual International Conference of the IEEE Engineering in Medicine & Biology Society (EMBC)*. IEEE, 2020, pp. 4749–4752.

[3] Y. Lai, S. Sutjipto, M. D. Clout, M. G. Carmichael, and G. Paul, "GAVRe2 : Towards Data-Driven Upper-Limb Rehabilitation with Adaptive-Feedback Gamification," in *2018 IEEE International Conference on Robotics and Biomimetics (ROBIO)*. IEEE, 2018, pp. 164–169.

[4] D. Leonardis, M. Barsotti, C. Loconsole, M. Solazzi, M. Troncossi, C. Mazzotti, V. P. Castelli, C. Procopio, G. Lamola, C. Chisari, M. Bergamasco, and A. Frisoli, "An EMG-controlled robotic hand exoskeleton for bilateral rehabilitation," *IEEE Transactions on Haptics*, vol. 8, no. 2, pp. 140–151, 2015.

[5] A. F. Salazar-Gomez, J. Delpreto, S. Gil, F. H. Guenther, and D. Rus, "Correcting robot mistakes in real time using EEG signals," in *Proceedings - IEEE International Conference on Robotics and Automation*. Institute of Electrical and Electronics Engineers Inc., 2017, pp. 6570–6577.

[6] B. Hudgins, P. Parker, and R. Scott, "A new strategy for multifunction myoelectric control," *IEEE Transactions on Biomedical Engineering*, vol. 40, no. 1, pp. 82–94, 1993.

[7] D. Bai, S. Chen, and J. Yang, "Upper arm motion high-density semg recognition optimization based on spatial and time-frequency domain features," *Journal of Healthcare Engineering*, vol. 2019, p. 3958029, Mar 2019. [Online]. Available: https://doi.org/10.1155/2019/3958029

[8] T. Petrič, L. Peternel, J. Morimoto, and J. Babič, "Assistive Arm-Exoskeleton Control Based on Human Muscular Manipulability," *Frontiers in Neurorobotics*, vol. 13, p. 30, 5 2019.

[9] M. G. Carmichael and D. Liu, "Estimating Physical Assistance Need Using a Musculoskeletal Model," *IEEE Transactions on Biomedical Engineering*, vol. 60, no. 7, pp. 1912–1919, 2013.

[10] F. M. Campos and J. M. Calado, "Approaches to human arm movement control-A review," *Annual Reviews in Control*, vol. 33, no. 1, pp. 69–77, 2009.

[11] E. B. Thorp, K. P. Kording, and F. A. Mussa-Ivaldi, "Using noise to shape motor learning," *Journal of Neurophysiology*, vol. 117, no. 2, pp. 728–737, 2017.

[12] A. L. Wong and A. M. Haith, "Motor planning flexibly optimizes performance under uncertainty about task goals," *Nature Communications*, vol. 8, no. 1, pp. 1–10, 2017.

[13] S. Sutjipto, M. G. Carmichael, and G. Paul, "Comparison of strength profile representations using musculoskeletal models and their applications in robotics," *Frontiers in Robotics and AI*, vol. 10, 2024. [Online]. Available: https://www.frontiersin.org/articles/10.3389/frobt.2023.1265635

[14] K. R. S. Holzbaur, W. M. Murray, and S. L. Delp, "A Model of the Upper Extremity for Simulating Musculoskeletal Surgery and Analyzing Neuromuscular Control," *Annals of Biomedical Engineering*, vol. 33, no. 6, pp. 829–840, 2005.

[15] K. R. Holzbaur, W. M. Murray, G. E. Gold, and S. L. Delp, "Upper limb muscle volumes in adult subjects," *Journal of Biomechanics*, vol. 40, no. 4, pp. 742–749, 2007.

[16] A. Seth, J. L. Hicks, T. K. Uchida, A. Habib, C. L. Dembia, J. J. Dunne, C. F. Ong, M. S. DeMers, A. Rajagopal, M. Millard, S. R. Hamner, E. M. Arnold, J. R. Yong, S. K. Lakshmikanth, M. A. Sherman, J. P. Ku, and S. L. Delp, "OpenSim: Simulating musculoskeletal dynamics and neuromuscular control to study human and animal movement," *PLoS Computational Biology*, vol. 14, no. 7, 2018.

[17] A. J. van den Bogert, T. Geijtenbeek, O. Even-Zohar, F. Steenbrink, and E. C. Hardin, "A real-time system for biomechanical analysis of human movement and muscle function," *Medical & Biological Engineering & Computing*, vol. 51, no. 10, pp. 1069–1077, 2013.

[18] A. Falisse, S. Van Rossom, J. Gijsbers, F. Steenbrink, B. J. van Basten, I. Jonkers, A. J. van den Bogert, and F. De Groote, "OpenSim Versus Human Body Model: A Comparison Study for the Lower Limbs During Gait," *Journal of Applied Biomechanics*, vol. 34, no. 6, pp. 496–502, 2018.

[19] D. G. Thelen, F. C. Anderson, and S. L. Delp, "Generating dynamic simulations of movement using computed muscle control," *Journal of Biomechanics*, vol. 36, no. 3, pp. 321–328, 2003.

[20] T. S. Buchanan, D. G. Lloyd, K. Manal, and T. F. Besier, "Estimation of muscle forces and joint moments using a forward-inverse dynamics model," *Medicine and science in sports and exercise*, vol. 37, no. 11, pp. 1911–1916, 2005.

[21] Y. C. Lin, T. W. Dorn, A. G. Schache, and M. G. Pandy, "Comparison of different methods for estimating muscle forces in human movement," *Journal of Engineering in Medicine*, vol. 226, no. 2, pp. 103–112, 2012.

[22] K. Stollenmaier, W. Ilg, and D. F. B. Haeufle, "Predicting Perturbed Human Arm Movements in a Neuro-Musculoskeletal Model to Investigate the Muscular Force Response," *Frontiers in Bioengineering and Biotechnology*, vol. 8, p. 308, 2020.

[23] J. L. Hicks, T. K. Uchida, A. Seth, A. Rajagopal, and S. L. Delp, "Is My Model Good Enough? Best Practices for Verification and Validation of Musculoskeletal Models and Simulations of Movement," *Journal of Biomechanical Engineering*, vol. 137, no. 2, p. 020905, 2015.

[24] J. F. Yang, J. P. Scholz, and M. L. Latash, "The role of kinematic redundancy in adaptation of reaching," *Experimental Brain Research*, vol. 176, no. 1, pp. 54–69, 2007.

[25] E. Todorov, "Optimality principles in sensorimotor control," *Nature Neuroscience*, vol. 7, no. 9, pp. 907–915, 2004.

[26] G. E. Loeb, "Optimal isn't good enough," *Biological Cybernetics*, vol. 106, no. 11-12, pp. 757–765, 2012.

[27] B. I. Prilutsky and V. M. Zatsiorsky, "Optimization-based models of muscle coordination," *Exercise and Sport Sciences Reviews*, vol. 30, no. 1, pp. 32–38, 2002.

[28] P. S. Glazier and S. Mehdizadeh, "In search of sports biomechanics' holy grail: Can athlete-specific optimum sports techniques be identified?" *Journal of Biomechanics*, vol. 94, pp. 1–4, 2019.

[29] J. D. Ortega and C. T. Farley, "Individual limb work does not explain the greater metabolic cost of walking in elderly adults," *Journal of Applied Physiology*, vol. 102, no. 6, pp. 2266–2273, 2007.

[30] D. A. Nowak, S. Glasauer, and J. Hermsdörfer, "How predictive is grip force control in the complete absence of somatosensory feedback?" *Brain*, vol. 127, no. 1, pp. 182–192, 2004.

[31] J. B. Heald, D. W. Franklin, and D. M. Wolpert, "Increasing muscle co-contraction speeds up internal model acquisition during dynamic motor learning," *Scientific Reports*, vol. 8, no. 1, 2018.

[32] D. W. Franklin and T. E. Milner, "Adaptive control of stiffness to stabilize hand position with large loads," *Experimental Brain Research*, vol. 152, no. 2, pp. 211–220, 9 2003.

[33] P. L. Gribble, L. I. Mullin, N. Cothros, and A. Mattar, "Role of cocontraction in arm movement accuracy," *Journal of Neurophysiology*, vol. 89, no. 5, pp. 2396–2405, 2003.

[34] D. Sternad, "It's not (only) the mean that matters: variability, noise and exploration in skill learning," *Current Opinion in Behavioral Sciences*, vol. 20, pp. 183–195, 4 2018.

[35] X. Chu, W. Yang, W. Ouyang, C. Ma, A. L. Yuille, and X. Wang, "Multi-context attention for human pose estimation," in *Proceedings - 30th IEEE Conference on Computer Vision and Pattern Recognition, CVPR 2017*, vol. 2017-January. IEEE, 2017, pp. 5669–5678.

[36] S. Corazza, L. Mündermann, A. M. Chaudhari, T. Demattio, C. Cobelli, and T. P. Andriacchi, "A markerless motion capture system to study musculoskeletal biomechanics: Visual hull and simulated annealing approach," *Annals of Biomedical Engineering*, vol. 34, no. 6, pp. 1019–1029, 2006.

[37] D. Stanev, K. Filip, D. Bitzas, S. Zouras, G. Giarmatzis, D. Tsaopoulos, and K. Moustakas, "Real-Time Musculoskeletal Kinematics and Dynamics Analysis Using Marker- and IMU-Based Solutions in Rehabilitation," *Sensors*, vol. 21, no. 5, p. 1804, 2021.

[38] M. G. Carmichael, S. Aldini, R. Khonasty, A. Tran, C. Reeks, D. Liu, K. J. Waldron, and G. Dissanayake, "The ANBOT: An Intelligent Robotic Co-worker for Industrial Abrasive Blasting," in *2019 IEEE/RSJ International Conference on Intelligent Robots and Systems (IROS)*. Macau, China: IEEE, 2019, pp. 8026–8033.

[39] T. Flash and N. Hogan, "The coordination of arm movements: An experimentally confirmed mathematical model," *Journal of Neuroscience*, vol. 5, no. 7, pp. 1688–1703, 1985.

[40] V. Mathiowetz, K. Weber, G. Volland, and N. Kashman, "Reliability and validity of grip and pinch strength evaluations," *Journal of Hand Surgery*, vol. 9, no. 2, pp. 222–226, 1984.

[41] R. Gurram, S. Rakheja, and G. J. Gouw, "A study of hand grip pressure distribution and EMG of finger flexor muscles under dynamic loads," *Ergonomics*, vol. 38, no. 4, pp. 684–699, 1995.

[42] S. Ambike, F. Paclet, V. M. Zatsiorsky, and M. L. Latash, "Factors affecting grip force: Anatomy, mechanics, and referent configurations," *Experimental Brain Research*, vol. 232, no. 4, pp. 1219–1231, 2014.

[43] J. J. Woods and B. Bigland-Ritchie, "Linear and non-linear surface EMG/force relationships in human muscles. An anatomical/functional argument for the existence of both," *American journal of physical medicine*, vol. 62, no. 6, pp. 287–99, 12 1983.

[44] A. Tran, D. Liu, R. Ranasinghe, M. Carmichael, and C. Liu, "Analysis of Human Grip Strength in Physical Human Robot Interaction," *Procedia Manufacturing*, vol. 3, pp. 1442–1449, 2015.

[45] S. Haddadin and E. Croft, "Physical Human-Robot Interaction," in *Springer Handbook of Robotics*, B. Siciliano and O. Khatib, Eds. Springer, Cham, 2016, ch. 69, pp. 1835–1874.

[46] T. J. Roberts and A. M. Gabaldón, "Interpreting muscle function from EMG: Lessons learned from direct measurements of muscle force," *Integrative and Comparative Biology*, vol. 48, no. 2, pp. 312–320, 2008.

[47] C. J. De Luca, "The Use of Surface Electromyography in Biomechanics," *Journal of Applied Biomechanics*, vol. 13, no. 2, pp. 135–163, 1997.

[48] National Center for Health Statistics, "NHANES Anthropometry Procedures Manual," 2020. [Online]. Available: https://wwwn.cdc.gov/nchs/data/nhanes/2019-2020/manuals/2020-Anthropometry-Procedures-Manual-508.pdf

[49] NIHR Southampton Biomedical Research Centre, "Procedure for Measruing ADULT ULNA LENGTH," 2014. [Online]. Available: https://www.uhs.nhs.uk/Media/Southampton-Clinical-Research/Procedures/BRCProcedures/Procedure-for-adult-ulna-length.pdf

[50] S. Rota, I. Rogowski, S. Champely, and C. Hautier, "Reliability of EMG normalisation methods for upper-limb muscles," *Journal of Sports Sciences*, vol. 31, no. 15, pp. 1696–1704, 2013.

[51] F. E. Zajac, "Muscle and tendon: properties, models, scaling, and application to biomechanics and motor control," *Critical reviews in biomedical engineering*, vol. 17, no. 4, pp. 359–411, 1989.

[52] A. V. Hill, "The heat of shortening and the dynamic constants of muscle," *Proceedings of the Royal Society of London. Series B - Biological Sciences*, vol. 126, no. 843, pp. 136–195, 1938.

[53] D. A. Winter, *Biomechanics and Motor Control of Human Movement*, 4th ed. Hoboken, NJ, USA: John Wiley & Sons, Inc., 9 2009.

[54] R. F. Chandler, C. E. Clauser, J. T. McConville, H. M. Reynolds, and J. W. Young, "Investigation of Inertial Properties of the Human Body," Aerospace Medical Research Laboratory, Tech. Rep., 1975.

[55] L. M. Schutte, M. M. Rodgers, F. E. Zajac, and R. M. Glaser, "Improving the Efficacy of Electrical Stimulation-Induced Leg Cycle Ergometry: An Analysis Based on a Dynamic Musculoskeletal Model," *IEEE Transactions on Rehabilitation Engineering*, vol. 1, no. 2, pp. 109–125, 6 1993.

[56] M. Millard, T. Uchida, A. Seth, and S. L. Delp, "Flexing computational muscle: Modeling and simulation of musculotendon dynamics," *Journal of Biomechanical Engineering*, vol. 135, no. 2, 2013.

[57] H. Krebs, J. Palazzolo, L. Dipietro, M. Ferraro, J. Krol, K. Rannekleiv, B. Volpe, and N. Hogan, "Rehabilitation Robotics: Performance-Based Progressive Robot-Assisted Therapy," *Autonomous Robots*, vol. 15, no. 1, pp. 7–20, 2003.